

On the sample-dependent minimal conductivity in weakly disordered graphene

Weiwei Chen,^{1,2} Yedi Shen,³ Bo Fu,⁴ Qinwei Shi,^{3,*} and W. Zhu^{2,1,†}

¹*Institute of Natural Sciences, Westlake Institute for Advanced Study, 18 Shilongshan Road, Hangzhou 310024, China*

²*School of Science, Westlake University, 18 Shilongshan Road, Hangzhou 310024, China*

³*Hefei National Laboratory for Physical Sciences at the Microscale,
and Synergetic Innovation Center of Quantum Information and Quantum Physics,
University of Science and Technology of China, Hefei, Anhui 230026, China*

⁴*Department of Physics, The University of Hong Kong, Pokfulam Road, Hong Kong, China*

(Dated: September 1, 2021)

We present a unified understanding for experimentally observed minimal dc conductivity at the Dirac point in weak disordered graphene. First of all, based on the linear response theory, we unravel that randomness or disorder, inevitably inducing momentum dependent corrections in electron self-energy function, naturally yields a sample-dependent minimal conductivity. Taking the long-ranged Gaussian potential as an example, we demonstrate the momentum dependent self-energy function within the Born approximation, and further validate it via numerical simulation using large-scale Lanczos algorithm. The explicit dependence of self-energy on the intensity, concentration and range of potential is critically addressed. Therefore, our results provide a reasonable interpretation of the sample-dependent minimal conductivity observed in graphene samples.

Introduction.—The early experimental measurements on graphene revealed a finite dc conductivity $\sigma_{\min} \approx \frac{4e^2}{h}$ at the Dirac point at low temperature [1–3], dubbed as minimal conductivity. Since experimental observations are larger than theoretical predicted value $\sigma_{\min} = \frac{4e^2}{\pi h}$ [4–6], giving rise to a famous “missing π ” problem [7]. To address this problem, recently more experiments have been carried out [2, 8–16], which show that the minimal conductivity is strongly sample-dependent and thus indicate the crucial role of randomness or disorder. The minimal conductivity measured in these experiments can be described as $\sigma_{\min} = C \frac{4e^2}{\pi h}$ with the factor C varying from 1.7 to 10, where the behavior of sample dependence is quite different from previous theoretical predictions.

Theoretical research on the minimal conductivity in two-dimensional disordered Dirac fermions has been intensively studied in the d-wave superconductivity in cuprate superconductors [17, 18] and the plateau transition in the integer quantum Hall effect [5]. The discovery of graphene [1–3] rejuvenated this problem. The previous theoretical results on σ_{\min} can be mainly summarized as: (i) scattering-independent value $\sigma_{\min} = \frac{4e^2}{\pi h}$ [4–6, 19–24], independent of strength and nature of disorder; (ii) a universal value $\sigma_{\min} = \frac{4e^2}{h}$, which is due to quantum criticality of graphene in the vicinity of Dirac point [25–27]; (iii) disorder-dependent σ_{\min} [6, 7, 28–34]. Especially, although some previous studies have obtained disordered-dependent minimal conductivity, most of which are based on semi-classical Boltzmann transport theory [6, 7, 28, 29], ignoring the disorder induced quantum corrections near the Dirac point. Since Boltzmann theory is not applicable around the Dirac point [7], a fully quantum mechanical treatment is highly desired to address the minimal conductivity.

Additionally, numerical calculations address this problem from various aspects [30–34]. Nomura and MacDonald numerically calculate σ_{\min} by finite-size Kubo formula and find that σ_{\min} is a few times larger for long-range Coulomb scatterers than for short-range scatterers [30]. Similar results are also

obtained by numerically calculating the transmission matrix [31, 32]. Noro *et al.* find that the minimal conductivity at the Dirac point remains universal in the clean limit, but increases with disorder and becomes non-universal for long-range scatterers through numerically solved self-energy and the current vertex function [33]. These numerical attempts urgently calls for a reasonable analytical interpretation of the minimal conductivity.

In this paper, we offer a general picture to understand the sample-dependent minimal conductivity. In the presence of long-ranged Gaussian potential, we elucidate that the self-energy is momentum-dependent, and in the vicinity of Dirac point the leading momentum-dependent correction is parameterized by a non-universal dimensionless parameter $\alpha = K_0 \frac{e^2 k^2}{8\pi}$ [Eq. (19)], which is determined by the disorder strength and the spatial range of the potential (details see below). Crucially, the electric minimal conductivity, evaluated via the standard Kubo formula by taking into account the corrected self-energy, obeys the relationship $\sigma_{\min} = \frac{1}{(1-\alpha)^2} \frac{4e^2}{\pi h}$ [Eq. (11)]. This finding, in sharp contrast to the disorder-independent value $\sigma_{\min} = \frac{4e^2}{\pi h}$ in previous studies [20, 24], provides a simple and physically appealing explanation for the observed minimum conductivity.

Minimal conductivity with momentum dependent self-energy.—The charge carriers of graphene near the half filling can be modeled by a Dirac Hamiltonian, describing a linear relation between energy and wave vector

$$H = \hbar v_f \boldsymbol{\sigma} \cdot \mathbf{k} \quad (1)$$

where $v_f \approx 10^6 \text{ ms}^{-1}$ is the Fermi velocity, $\boldsymbol{\sigma} = (\sigma_x, \sigma_y)$ are the Pauli matrices of pseudospin (sublattice), and $\mathbf{k} = (k_x, k_y)$ is a two-component wave vector. The eigenvalues and eigenstates of Hamiltonian Eq. (1) are

$$E_{\mathbf{k}s} = s\hbar v_f k; \quad \Psi_{\mathbf{k}s}(\mathbf{r}) = \langle \mathbf{r} | \mathbf{k}s \rangle = \frac{e^{i\mathbf{k} \cdot \mathbf{r}}}{\sqrt{2\mathcal{V}}} \begin{pmatrix} 1 \\ s e^{i\theta_{\mathbf{k}}} \end{pmatrix} \quad (2)$$

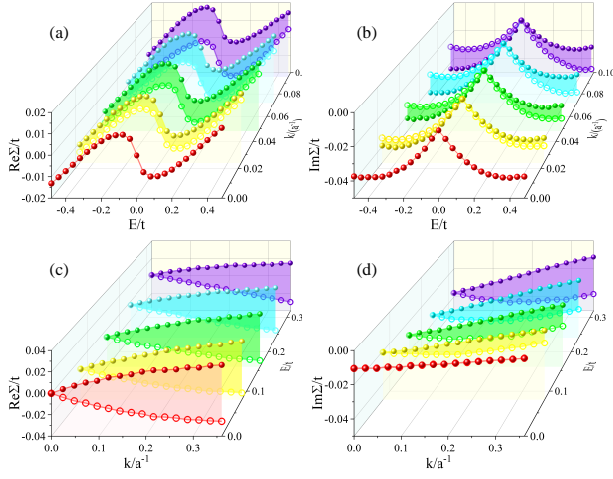


FIG. 1. (a-b) Numerical results of real and imaginary part of self-energy versus Fermi energy with different momentum: $k = 0$ (red), $k = 0.024/a$ (yellow), $k = 0.048/a$ (green), $k = 0.072/a$ (cyan), $k = 0.096/a$ (purple). (c-d) Numerical results of real and imaginary part of self-energy versus momentum with different Fermi energy: $E = 0$ (red), $E = 0.08t$ (yellow), $E = 0.16t$ (green), $E = 0.24t$ (cyan), $E = 0.32t$ (purple). Lines with solid dots denote subband with $s = -1$ while lines with open dots denote $s = 1$. Here we set impurity concentration $n_{\text{imp}} = 5\%$, correlation length $\xi = 3.6a$, impurity strength $u_0 = 0.16t$. A global dependence of self-energy on k, E is shown in the supplemental materials [41].

where $s = \pm$ denotes the band index ($s = +1$ for the conduction band and $s = -1$ for the valence band), \mathcal{V} is the area of sample, and $\theta_{\mathbf{k}} = \arctan(k_y/k_x)$ is the angle of wave vector \mathbf{k} down from the positive x -axis. The velocity $\frac{1}{\hbar} \frac{\partial H}{\partial k_x}$ along the x direction in eigenstates basis is

$$v_x(\mathbf{k}) = v_f(\cos \theta_{\mathbf{k}} \sigma_z + \sin \theta_{\mathbf{k}} \sigma_y). \quad (3)$$

In general, the electron self-energy induced by the impurity scattering is both momentum- and energy-dependent. For short-ranged disorder potential, the momentum dependence in self-energy is negligible [4–7]. For long-range disorder potential, the self-energy is commonly treated in the on-shell approximation ($E = E_{\mathbf{k}s}$) [35], i.e. the momentum dependence of the self-energy is replaced by the single-particle energy in clean limit. However, the numerical calculations that we will present below show that self-energy near the Dirac point is indeed dependent on the momentum. Therefore, we assume the self-energy function can be separated into a energy-dependent and a static momentum-dependent contribution,

$$\Sigma(\mathbf{k}s, E) \approx \Sigma_1(E) - \alpha s \hbar v_f k + i \Sigma_2(E) \quad (4)$$

where $s = \pm$ is the band index, $\Sigma_1(E)$ and $\Sigma_2(E)$ describe the energy-dependent terms in real part and imaginary part. Since the long-ranged random scalar disorder we considered does not break up the particle-hole symmetry on average [20, 36–38], the self-energy in the eigenstate basis satisfies relations, $\text{Re}\Sigma(\mathbf{k}+, E) = -\text{Re}\Sigma(\mathbf{k}-, -E)$ and $\text{Im}\Sigma(\mathbf{k}+, E) =$

$\text{Im}\Sigma(\mathbf{k}-, -E)$, which preserve the dispersion relation and broaden width of conduction and valence bands symmetric about the Dirac point [39].

Now we study the influence of this momentum dependent self-energy function on the minimal conductivity. Based on linear response theory, we can calculate the longitudinal conductivity at zero temperature by the Kubo formula [40]

$$\sigma_{xx}(E) = \sigma_{xx}^{RA}(E) - \text{Re}[\sigma_{xx}^{RR}(E)] \quad (5)$$

with

$$\sigma_{xx}^{RA}(E) = 4 \frac{e^2 \hbar}{2\pi \mathcal{V}} \text{Tr} [G^R(E) v_x G^A(E) v_x] \quad (6)$$

$$\sigma_{xx}^{RR}(E) = 4 \frac{e^2 \hbar}{2\pi \mathcal{V}} \text{Tr} [G^R(E) v_x G^R(E) v_x] \quad (7)$$

Here the factor 4 denotes degeneracy of real spin and valley and $\text{Tr}[\dots]$ means the trace over both wave vector and pseudospin (sublattice) spaces. $G^{R/A}(E)$ is the full retarded/advanced Green's function. In the eigenstate basis, it is

$$G^{R/A}(\mathbf{k}, E) = \begin{pmatrix} g_+^{R/A}(\mathbf{k}, E) & 0 \\ 0 & g_-^{R/A}(\mathbf{k}, E) \end{pmatrix} \quad (8)$$

where

$$g_s^{R/A}(\mathbf{k}, E) = \frac{1}{a - (1 - \alpha) s \hbar v_f k \pm i \eta}, \quad \begin{cases} a = E - \Sigma_1(E) \\ \eta = -\Sigma_2(E) \end{cases} \quad (9)$$

Plugging Eq. (3), Eq. (8) and Eq. (9) into Kubo formula Eq. (5), we obtain the conductivity

$$\sigma_{xx}(E) = \frac{2e^2}{\pi \hbar} \frac{1}{(1 - \alpha)^2} \left(1 + \frac{a}{\eta} \arctan \frac{a}{\eta} \right) + \frac{2e^2}{\pi \hbar} \frac{1}{(1 - \alpha)^2} \frac{\eta}{a} \arctan \frac{a}{\eta} \quad (10)$$

where the first and second term denote the electron-hole incoherent and coherent contribution respectively. At the Dirac point ($E = 0$), these two parts contribute equally and the minimal conductivity is arrived as

$$\sigma_{\text{min}} = \frac{1}{(1 - \alpha)^2} \frac{4e^2}{\pi \hbar}. \quad (11)$$

Here we would like to give some remarks. First, Eq. (11) contains both electron-hole coherent and incoherent contributions, which is beyond the traditional Boltzmann transport theory where electron-hole incoherent contribution from the retarded-retarded (RR) channel is usually discarded. Second, the vertex correction is analyzed in the supplemental materials [41] which shows the influence of vertex correction is much smaller than the change caused by momentum-dependent self-energy at the level of the bubble diagram. This is consistent with the previous works that the vertex correction is negligible for calculation of minimal conductivity [6, 18]. A plausible explanation is that the forward and back scattering are exactly complementary in the electron-hole incoherent and coherent contributions for isotropic disorder potential at Dirac

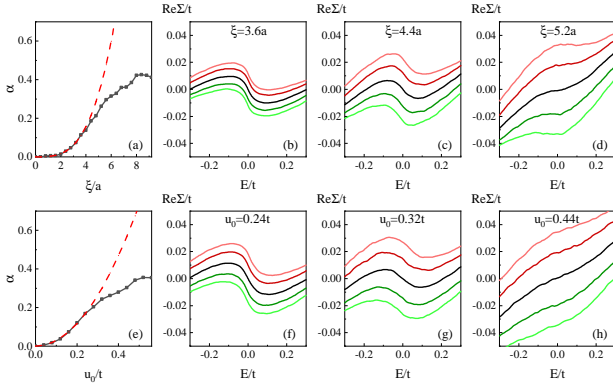


FIG. 2. (a) α versus ξ with $n_{\text{imp}} = 5\%$ and $u_0 = 0.16t$. (b)-(d) Real part of self-energy $\text{Re}\Sigma$ for different $\xi = 3.6a$ (b), $4.4a$ (c), and $5.2a$ (d). (e) α versus u_0 with $n_{\text{imp}} = 5\%$ and $\xi = 3.2a$. (f)-(h) Real part of self-energy $\text{Re}\Sigma$ for different $u_0 = 0.24t$ (f), $0.32t$ (g), and $0.44t$ (h). The dashed lines in (a,e) are fitting curves to the numerical data, which are $\alpha = 1.6(\xi/a)^{3.3} \times 10^{-3}$ and $\alpha = 2.9(u_0/t)^2$. In (b-d) and (f-h), colors label various momenta: Dirac point $k = 0$ (black), $k = 0.048/a$ and $s = -1$ (red), $k = 0.096/a$ and $s = -1$ (light red), $k = 0.048/a$ and $s = 1$ (green), $k = 0.096/a$ and $s = 1$ (light green).

point, while the vertex correction enhances the back scattering and weakens the forward scattering. Third, from the result Eq. (11), it is clear that the minimal conductivity σ_{min} is independent on the energy-dependent part in the self-energy function, i.e. $\Sigma_1(E)$ and $\Sigma_2(E)$, if they satisfy the limit condition, $\frac{a}{\eta} \rightarrow 0$ when $E \rightarrow 0$, but σ_{min} is significantly influenced by the momentum dependent term. This behavior explains why majority of previous theoretical studies predicted $\sigma_{\text{min}} = \frac{4e^2}{\pi h}$, independent with strength and nature of disorder [4, 5, 23]. Fourth, for the long range disorder, previous calculations within the self-consistent Born approximation reported the momentum contribution to self-energy function, however, the role of this term on transport was unfortunately washed out in the widely-used on-shell approximation [20]. Finally, with all of these non-trivial improvements, we point out that Eq. (11) shows the minimal conductivity is enhanced by disorder, in contrast to those from Boltzmann theory [6, 28, 29]. One interpretation is that the presence of potential fluctuations smooth on the scale of the graphene lattice spacing increases the conductivity through quantum interference effects [30–35].

Estimation of α by the Born approximation—In order to incorporate insights of the momentum dependent self-energy theoretically, we take long-ranged Gaussian potential, as an example, with zero mean and correlation function as

$$\mathcal{K}(\mathbf{r} - \mathbf{r}') = \langle U(\mathbf{r})U(\mathbf{r}') \rangle = K_0 \frac{(\hbar v_f)^2}{2\pi\xi^2} e^{-|\mathbf{r}-\mathbf{r}'|^2/2\xi^2} \quad (12)$$

where ξ is the correlation length and K_0 is a dimensionless parameter that parametrizes its magnitude. Its Fourier transformation form is

$$\mathcal{K}(\mathbf{q}) = \int d\mathbf{r} \mathcal{K}(\mathbf{r}) e^{-i\mathbf{q}\cdot\mathbf{r}} = K_0 (\hbar v_f)^2 e^{-\frac{\xi^2 \mathbf{q}^2}{2}}. \quad (13)$$

Based on the Born approximation, the self-energy is

$$\Sigma^B(\mathbf{k}s, E) = \sum_{s'} \int \frac{d^2\mathbf{k}'}{(2\pi)^2} \mathcal{K}(\mathbf{k} - \mathbf{k}') G_0^R(\mathbf{k}'s', E) \frac{1 + s's' \cos \theta}{2} \quad (14)$$

where $G_0^R(\mathbf{k}'s', E) = (E - s'\hbar v_f k' + i0^+)^{-1}$ is the Green's function of clean system in eigenstate basis, $\theta = \theta_{\mathbf{k}} - \theta_{\mathbf{k}'}$ is the angle between wave vector \mathbf{k} and \mathbf{k}' . In the following, we separate the calculation of self-energy function into real and imaginary parts, by using the Sokhotsky's formula, $\frac{1}{x+i0^+} = \mathcal{P}\frac{1}{x} - i\pi\delta(x)$, where \mathcal{P} denotes Cauchy principal value.

The imaginary part of self-energy can be solved as

$$\text{Im}\Sigma^B(\mathbf{k}s, E) = -\frac{K_0}{4}|E|e^{-\frac{\xi^2}{2}\left(k^2 + \frac{E^2}{\hbar^2 v_f^2}\right)} \left[I_0\left(\frac{\xi^2 k E}{\hbar v_f}\right) + s I_1\left(\frac{\xi^2 k E}{\hbar v_f}\right) \right] \quad (15)$$

where $I_0(x)$ and $I_1(x)$ are the zero and first order of modified Bessel functions of the first kind [42, 43]. In the meanwhile, the real part of self-energy is obtained as

$$\begin{aligned} \text{Re}\Sigma^B(\mathbf{k}s, E) &= \frac{K_0(\hbar v_f)^2}{4\pi} \mathcal{P} \int_{-k_c}^{k_c} dk' k' e^{-\frac{\xi^2}{2}(k^2 + k'^2)} \\ &\times \frac{I_0(\xi^2 k k') + s I_1(\xi^2 k k')}{E - \hbar v_f k'}. \end{aligned} \quad (16)$$

Focusing on the Dirac physics, we assume $\frac{|E|}{\hbar v_f}, k \ll \frac{1}{\xi}$ and obtain the self-energy in powers of k and E ,

$$\text{Im}\Sigma^B(\mathbf{k}s, E) = -\frac{K_0}{4}|E| + \dots \quad (17)$$

$$\text{Re}\Sigma^B(\mathbf{k}s, E) = \frac{K_0}{2\pi} E \ln \left| \frac{E}{\hbar v_f k_c} \right| + \alpha E - \alpha s \hbar v_f k + \dots \quad (18)$$

where \dots stand for terms in order of $O(kE^2, k^2E, E^3)$ in imaginary part and $O(kE^2 \ln E, k^2E \ln E, E^3 \ln E)$ in real part. From this result, a momentum linear dependent term is controlled by a dimensionless coefficient

$$\alpha = K_0 \frac{\xi^2 k_c^2}{8\pi}. \quad (19)$$

Importantly, under the on-shell approximation ($E = E_{\mathbf{k}s} = s\hbar v_f k$), the momentum dependent correction in Eq. (18) vanishes, thus we recover the previous results [6, 7, 35].

Here we stress that, the Born approximation or self-consistent Born approximation, which has been widely used in existing literatures, is always applied together with on-shell approximation, so that the momentum and energy dependence of the self-energy in these works are not isolated [28, 33, 35]. Our findings show that in the low energy regime the on-shell approximation is not well justified, i.e. the momentum and energy dependence in the self-energy are decoupled as shown in Eqs. (17) and (18). Moreover, we find the momentum dependent terms are less important in the imaginary part of self-energy than those in the real part, because they are at least two orders higher than the leading term in the imaginary part. Furthermore, our results can recover those predictions in the existing literatures under the on-shell approximation at the regime far away from the Dirac point, where the

imaginary part of self-energy is a constant independent of energy and momentum, and real part of self-energy disappears [4, 35, 41, 44].

Numerical Simulations.—Next we turn to numerical simulations by Lanczos recursive method [45], using a large supercell with $N = 2400 \times 2400 \times 2$ atoms and periodic boundary condition. The long-ranged Gaussian potential is chosen by $U(\mathbf{r}) = \sum_{n=i}^{N_{\text{imp}}} \pm u_0 e^{-|\mathbf{r}-\mathbf{R}_n|^2/\xi^2}$, where \mathbf{R}_n and N_{imp} are the location and total number of impurity and impurities of $\pm u_0$ are randomly distributed with equal probability. In this case, the dimensionless parameter K_0 in the correlation function Eq. (12) has different expressions for sharp ($\xi \ll a$) and smooth ($\xi \gg a$) potential [32, 33, 46, 47]

$$K_0 = \frac{n_{\text{imp}} u_0^2}{(\hbar v_f)^2} \times \begin{cases} \frac{A_c}{2}; & \xi \ll a \\ \frac{2\pi^2}{A_c} \xi^4; & \xi \gg a \end{cases} \quad (20)$$

where $a = 1.42\text{\AA}$ the carbon-carbon distance of graphene, $A_c = \frac{3}{2}a^2$ is the area of primitive cell, and $n_{\text{imp}} = N_{\text{imp}}/N$ is impurity concentration.

In the Fig. 1, we display the self-energy functions versus Fermi energy and momentum. Obviously, self-energy not only depends on Fermi energy, but also on momentum. As shown in $E - \text{Re}\Sigma$ plane of Fig. 1 (a), the momentum dependence of real part of self-energy function is significant in the low-energy region and gradually disappears with the increase of energy, while the situation is opposite for the imaginary part in $E - \text{Im}\Sigma$ plane of Fig. 1 (b). Then from the curves in $k - \text{Re}\Sigma$ plane of Fig. 1 (c), we see that the real part of self-energy function near the Dirac point is linearly related to the momentum, and the coefficient of the two eigenbands $s = \pm 1$ are opposite. These behaviors mean that the Born estimation [Eq. (18)] without on-shell approximation is reasonable around the Dirac point, thus we can assume the self-energy as Eq. (4).

In Figures 2 (a)-(d), we exhibit the effect of the correlation length ξ on the momentum dependence of real part of self-energy. When disorder strength is small, α has a positive relation with ξ , which can be fitted as $\alpha = 1.6(\xi/a)^{3.3} \times 10^{-3}$. This result is roughly consistent with Born approximation which predicts: $\alpha \propto \xi^2$ at the limit $\xi \ll a$ and $\alpha \propto \xi^6$ at the limit $\xi \gg a$ according to the Eqs. (19) and (20). With the further increasing of ξ , the value of α tends to saturate and eventually decrease. This behavior indicates the Born approximation tends to be invalid when deviating from the weak-scattering limit, since the increase of ξ also enhances the disorder strength K_0 .

In Figures 2 (f)-(h), we exhibit the effect of the impurity strength u_0 . Similar to the correlation length, we fit the relation of ξ and α in weak disorder regime, and obtain $\alpha = 2.9(u_0/t)^2$. This result has a good agreement with the prediction of Born approximation: $\alpha \propto K_0 \propto u_0^2$.

In addition, from Fig. 2 (b)-(d) and (f)-(h), we find that the momentum dependence of the self-energy gradually decreases at the high energy, where the on-shell approximation tends to be valid. The numerical simulation at the limit $k, \frac{E}{\hbar v_f} \ll \frac{1}{\xi}$ is

further addressed in the Supp. Mat. [41].

Conclusion.—We have shown that the momentum dependent correction to the self-energy function is of paramount importance for transport properties of disordered Dirac fermions. We reveal momentum dependent self-energy produces a non-universal minimal conductivity. Furthermore, we elaborate the origin of this momentum dependent correction analytically and uncover its dependence on disorder potential, which is also verified by unbiased numerical simulations.

Finally, our findings offer a intuition to understand the existing numerical simulations [30, 31, 46] where Coulomb impurities enhance the minimal conductivity. Additionally, as long-range potentials can produce sample-dependent minimal conductivity, it suggests long-ranged scatters could be the dominant microscopic source of remnant disorder in ultrahigh-mobility graphene, in line with the experimental observations [14]. As a typical estimation for experimental condition [16, 35, 48] $K_0 \approx 1$ and $\alpha \approx 0.4$, we have $\sigma_{\text{min}} \approx 3.5e^2/h$, largely in agreement with measured values.

This work has received funding from the Project 12047544 supported by National Natural Science Foundation of China.

* Corresponding author. E-mail: phsqw@ustc.edu.cn

† Corresponding author. E-mail: zhuwei@westlake.edu.cn

- [1] K. S. Novoselov, A. K. Geim, S. V. Morozov, D. Jiang, M. I. Katsnelson, I. V. Grigorieva, S. V. Dubonos, and A. A. Firsov, *Nature* (London). **438**, 197 (2005).
- [2] Y. Zhang, Y.-W. Tan, H. L. Stormer, and Philip Kim, *Nature* (London). **438**, 201 (2005).
- [3] K. S. Novoselov, D. Jiang, F. Schedin, T. J. Booth, V. V. Khotkevich, S. V. Morozov, and A. K. Geim, *Proc. Natl. Acad. Sci. USA* **102**, 10451 (2005).
- [4] A. A. Nersisyan, A. M. Tselik, and F. Wenger, *Phys. Rev. Lett.* **72**, 2628 (1994).
- [5] A. W. W. Ludwig, M. P. Fisher, R. Shankar, and G. Grinstein, *Phys. Rev. B* **50**, 7526 (1994).
- [6] N. H. Shon and T. Ando, *J. Phys. Soc. Jpn.* **67**, 2421 (1998).
- [7] S. Das Sarma, Shaffique Adam, E. H. Hwang, and Enrico Rossi, *Rev. Mod. Phys.* **83**, 407 (2011).
- [8] K. I. Bolotin, K. J. Sikes, J. Hone, H. L. Stormer, and P. Kim, *Phys. Rev. Lett.* **101**, 096802 (2008).
- [9] X. Du, I. Skachko, A. Barker, and E. Y. Andrei, *Nat. Nanotech.* **3**, 491 (2008).
- [10] S. V. Morozov, K. S. Novoselov, M. I. Katsnelson, F. Schedin, D. C. Elias, J. A. Jaszczak, and A. K. Geim, *Phys. Rev. Lett.* **100**, 016602 (2008).
- [11] C. R. Dean, A. F. Young, I. Meric, C. Lee, L. Wang, S. Sorgenfrei, K. Watanabe, T. Taniguchi, P. Kim, K. L. Shepard, and J. Hone, *Nat. Nanotechnol.* **5**, 722 (2010).
- [12] P. J. Zomer, S. P. Dash, N. Tombros, and B. J. van Wees, *Appl. Phys. Lett.* **99**, 232104 (2011).
- [13] A. S. Mayorov, D. C. Elias, I. S. Mukhin, S. V. Morozov, L. A. Ponomarenko, K. S. Novoselov, A. K. Geim, and R. V. Gorbachev, *Nano Lett.* **12**, 4629 (2012).
- [14] N. J. G. Couto, D. Costanzo, S. Engels, D. K. Ki, K. Watanabe, T. Taniguchi, C. Stampfer, F. Guinea, and A. F. Morpurgo, *Phys. Rev. X* **4**, 041019 (2014).

- [15] L. J. Wang, P. Makk, S. Zihlmann, A. Baumgartner, D. I. Indolese, K. Watanabe, T. Taniguchi, and C. Schonberger, *Phys. Rev. Lett.* **124**, 157701 (2020).
- [16] Y.-W. Tan, Y. Zhang, K. Bolotin, Y. Zhao, S. Adam, E. H. Hwang, S. Das Sarma, H. L. Stormer, and P. Kim, *Phys. Rev. Lett.* **99**, 246803 (2007).
- [17] P. A. Lee, *Phys. Rev. Lett.* **71**, 1887 (1993).
- [18] A. C. Durst and P. A. Lee, *Phys. Rev. B* **62**, 1270 (2000).
- [19] N. M. R. Peres, F. Guinea, and A. H. Castro Neto, *Phys. Rev. B* **73**, 125411 (2006).
- [20] P. M. Ostrovsky, I. V. Gornyi, A. D. Mirlin, *Phys. Rev. B* **74**, 235443 (2006).
- [21] M. I. Katsnelson, *Eur. Phys. J. B* **51**, 157 (2006).
- [22] J. Tworzydło, B. Trauzettel, M. Titov, A. Rycerz, and C. W. J. Beenakker, *Phys. Rev. Lett.* **96**, 246802 (2006).
- [23] K. Ziegler, *Phys. Rev. B* **75**, 233407 (2007).
- [24] A. A. Fedorenko, D. Carpentier, and E. Orignac, *Phys. Rev. B* **85**, 125437 (2012).
- [25] P. M. Ostrovsky, I. V. Gornyi, and A. D. Mirlin, *Eur. Phys. J. Spec. Top.* **148**, 63 (2007).
- [26] P. M. Ostrovsky, I. V. Gornyi, and A. D. Mirlin, *Phys. Rev. Lett.* **98**, 256801 (2007).
- [27] A. Schuessler, P. M. Ostrovsky, I. V. Gornyi, and A. D. Mirlin, *Phys. Rev. B* **79**, 075405 (2009).
- [28] M. Trushin and J. Schliemann, *Phys. Rev. Lett.* **99**, 216602 (2007).
- [29] S. Adam, E. H. Hwang, V. M. Galitski, and S. Das Sarma, *Proc. Natl. Acad. Sci. USA* **104**, 18392 (2009).
- [30] K. Nomura and A. H. MacDonald, *Phys. Rev. Lett.* **98**, 076602 (2007).
- [31] J. H. Bardarson, J. Tworzydło, P.W. Brouwer, and C.W. J. Beenakker, *Phys. Rev. Lett.* **99**, 106801 (2007).
- [32] A. Rycerz, J. Tworzydło, and C. W. J. Beenakker, *Europhys. Lett.* **79** (2007) 57003.
- [33] M. Noro, M. Koshino, and T. Ando, *J. Phys. Soc. Jpn* **79**, 094713 (2010).
- [34] T. M. Radchenko, A. A. Shylau, and I. V. Zozoulenko, *Phys. Rev. B* **86**, 035418 (2012).
- [35] S. Adam, P. W. Brouwer, and S. Das Sarma, *Phys. Rev. B* **79**, 201404(R) (2009).
- [36] E. Fradkin, *Phys. Rev. B* **33**, 3257 (1986); *ibid.* **33**, 3263 (1986).
- [37] I. L. Aleiner, K. B. Efetov, *Phys. Rev. Lett.* **97**, 236801 (2006).
- [38] A. Altland and M. R. Zirnbauer, *Phys. Rev. B* **55**, 1142 (1997).
- [39] Ben Yu-Kuang Hu, E. H. Hwang, and S. Das Sarma, *Phys. Rev. B* **78**, 165411 (2008).
- [40] H. Bruus and C. Flensberg, *Many-Body Quantum Theory in Condensed Matter Physics* (Oxford University Press, New York, 2004).
- [41] See Supplemental Materials at <http://link.aps.org/supplemental>
- [42] I. Gradshteyn and I. Ryzhik, *Table of Integrals, Series, and Products*, 7th ed. (Academic, New York, 2007).
- [43] M. Abramowitz and I. A. Stegun, *Handbook of Mathematical Functions With Formulas, Graphs, and Mathematical Tables*, 10th ed. (National Bureau of Standards, 1972).
- [44] E. McCann, K. Kechedzhi, Vladimir I. Fal'ko, H. Suzuura, T. Ando, and B. L. Altshuler, *Phys. Rev. Lett.* **97**, 146805 (2006).
- [45] W. Chen, C. Xiao, Q. Shi, and Q. Li, *Phys. Rev. B* **101**, 020203 (2020).
- [46] J. W. Kłos and I. V. Zozoulenko, *Phys. Rev. B* **82**, 081414(R) (2010).
- [47] Z. Fan, J. H. Garcia, A. W. Cummings, J. E. Barrios-Vargas, M. Panhans, A. Harju, F. Ortman, and S. Roche, *Phys. Rep.* **903** (2020), 1-69.
- [48] S. Adam, S. Cho, M. S. Fuhrer, and S. Das Sarma, *Phys. Rev. Lett.* **101**, 046404 (2008).

Supplemental materials for “On the sample-dependent minimal conductivity in weakly disordered graphene”

Weiwei Chen

*Institute of Natural Sciences, Westlake Institute for Advanced Study,
18 Shilongshan Road, Hangzhou 310024, China and
School of Science, Westlake University, 18 Shilongshan Road, Hangzhou 310024, China*

Yedi Shen and Qinwei Shi*

*Hefei National Laboratory for Physical Sciences at the Microscale,
and Synergetic Innovation Center of Quantum Information and Quantum Physics,
University of Science and Technology of China, Hefei, Anhui 230026, China*

Bo Fu

Department of Physics, The University of Hong Kong, Pokfulam Road, Hong Kong, China

W. Zhu[†]

*School of Science, Westlake University, 18 Shilongshan Road, Hangzhou 310024, China and
Institute of Natural Sciences, Westlake Institute for Advanced Study, 18 Shilongshan Road, Hangzhou 310024, China*

In this supplementary, we detail the analytical derivation of self-energy function of graphene suffering long-ranged Gaussian disorder potential using Born approximation, display the global numerical result of self-energy function depending on momentum k and energy E , compare the numerical result of self-energy function with the analytical prediction at the limit $k, E \gg \frac{1}{\xi}$, and exhibit the calculation of bubble diagram and vertex correction of dc conductivity in detail.

ANALYTICAL DERIVATION OF SELF-ENERGY FUNCTION

We evaluate the self-energy function in the present of long ranged Gaussian potential by Born approximation:

$$\begin{aligned}\Sigma^B(\mathbf{k}, E) &= \frac{1}{\mathcal{V}^2} \sum_{\mathbf{k}'} \overline{|V(\mathbf{k} - \mathbf{k}')|^2} U_{\mathbf{k}}^\dagger U_{\mathbf{k}'} G_0^R(\mathbf{k}', E) U_{\mathbf{k}'}^\dagger U_{\mathbf{k}} \\ &= \frac{1}{2} \int \frac{d^2 \mathbf{k}'}{(2\pi)^2} \mathcal{K}(\mathbf{k} - \mathbf{k}') \begin{pmatrix} (g_0^+ + g_0^-) + \cos \theta (g_0^+ - g_0^-) & i \sin \theta (g_0^+ - g_0^-) \\ -i \sin \theta (g_0^+ - g_0^-) & (g_0^+ + g_0^-) - \cos \theta (g_0^+ - g_0^-) \end{pmatrix}\end{aligned}\quad (S1)$$

where $\theta = \theta_{\mathbf{k}} - \theta_{\mathbf{k}'}$ is the angle between momentum \mathbf{k} and \mathbf{k}' , and $g_0^\pm = G_0^R(\mathbf{k}' \pm, E) = 1/(E + i\eta - E_{\mathbf{k}' \pm})$ is the retarded Green's function for eigenstate with momentum \mathbf{k}' and chiral $s = \pm 1$. Based on the parity analysis, we find the integral of off-diagonal term is vanishing so that the first-order self-energy function in eigenstates basis can be expressed as

$$\Sigma^B(\mathbf{k}s, E) = \sum_{s'} \int \frac{d^2 \mathbf{k}'}{(2\pi)^2} \mathcal{K}(\mathbf{k} - \mathbf{k}') G_0^R(\mathbf{k}'s', E) \frac{1 + ss' \cos \theta}{2} \quad (S2)$$

which is the Eq.(14) in the main paper. After plugging the expression of $\mathcal{K}(\mathbf{k} - \mathbf{k}')$ into this equation, it is obtained

$$\Sigma^B(\mathbf{k}s, E) = K_0 (\hbar v_f)^2 \sum_{s'} \int \frac{d^2 \mathbf{k}'}{(2\pi)^2} e^{-\frac{\xi^2 (\mathbf{k} - \mathbf{k}')^2}{2}} G_0^R(\mathbf{k}'s', E) \frac{1 + ss' \cos \theta}{2} \quad (S3)$$

For $E > 0$, the imaginary part of the self-energy is

$$\begin{aligned}\text{Im} \Sigma^B(\mathbf{k}s, E) &= K_0 (\hbar v_f)^2 \sum_{s'} \int \frac{d^2 \mathbf{k}'}{(2\pi)^2} e^{-\frac{\xi^2 (\mathbf{k} - \mathbf{k}')^2}{2}} \frac{1 + ss' \cos \theta}{2} [-\pi \delta(E - s' \hbar v_f k')] \\ &= -\frac{\pi K_0 \hbar v_f}{2} \sum_{s'} \int \frac{k' dk' d\theta}{(2\pi)^2} e^{-\frac{\xi^2 (k^2 + k'^2 - 2kk' \cos \theta)}{2}} (1 + ss' \cos \theta) \delta\left(\frac{E}{\hbar v_f} - s' k'\right) \\ &= -\frac{K_0}{8\pi} E e^{-\frac{\xi^2}{2} \left(k^2 + \frac{E^2}{\hbar^2 v_f^2}\right)} \int_{-\pi}^{\pi} d\theta e^{\frac{\xi^2 k E}{\hbar v_f} \cos \theta} (1 + s \cos \theta) \\ &= -\frac{K_0}{4} E e^{-\frac{\xi^2}{2} \left(k^2 + \frac{E^2}{\hbar^2 v_f^2}\right)} \left[I_0\left(\frac{\xi^2 k E}{\hbar v_f}\right) + s I_1\left(\frac{\xi^2 k E}{\hbar v_f}\right) \right]\end{aligned}\quad (S4)$$

where $\tilde{E} = \frac{E}{\hbar v_f}$. In the final expression above, we have introduced modified Bessel functions of the first kind, whose integral representation is

$$I_\alpha(z) = \frac{1}{\pi} \int_0^\pi e^{z \cos \theta} \cos \alpha \theta d\theta - \frac{\sin \alpha \pi}{\pi} \int_0^\infty e^{-z \cosh t - \alpha t} dt \quad (S5)$$

and has series expansion,

$$I_\alpha(z) = \sum_{m=0}^{\infty} \frac{1}{m! \Gamma(m + \alpha + 1)} \left(\frac{z}{2}\right)^{2m + \alpha}, \quad (S6)$$

asymptotic expansion for large z ,

$$I_\alpha(z) = \frac{1}{\sqrt{2\pi z} \sqrt[4]{1 + \frac{\alpha^2}{z^2}}} \exp \left[-\alpha \text{arsinh} \left(\frac{\alpha}{z} \right) + z \sqrt{1 + \frac{\alpha^2}{z^2}} \right] \left[1 + o \left(\frac{1}{z \sqrt{1 + \frac{\alpha^2}{z^2}}} \right) \right]. \quad (S7)$$

Similarly, for $E < 0$, the imaginary part of the self-energy is

$$\begin{aligned}
\text{Im}\Sigma^B(\mathbf{k}s, E) &= K_0(\hbar v_f)^2 \sum_{s'} \int \frac{d^2\mathbf{k}'}{(2\pi)^2} e^{-\frac{\xi^2(\mathbf{k}-\mathbf{k}')^2}{2}} \frac{1 + ss' \cos \theta}{2} [-\pi \delta(E - s'\hbar v_f k')] \\
&= -\frac{\pi K_0 \hbar v_f}{2} \sum_{s'} \int \frac{k' dk' d\theta}{(2\pi)^2} e^{-\frac{\xi^2(k^2+k'^2-2kk' \cos \theta)}{2}} (1 + ss' \cos \theta) \delta\left(\frac{E}{\hbar v_f} - s'k'\right) \\
&= \frac{K_0}{8\pi} E e^{-\frac{\xi^2}{2}\left(k^2 + \frac{E^2}{\hbar^2 v_f^2}\right)} \int_{-\pi}^{\pi} d\theta e^{-\frac{\xi^2 k E \cos \theta}{\hbar v_f}} (1 - s \cos \theta) \\
&= \frac{K_0}{4} E e^{-\frac{\xi^2}{2}\left(k^2 + \frac{E^2}{\hbar^2 v_f^2}\right)} \left[I_0\left(-\frac{\xi^2 k E}{\hbar v_f}\right) - s I_1\left(-\frac{\xi^2 k E}{\hbar v_f}\right) \right]
\end{aligned} \tag{S8}$$

Combining two conditions, we can get

$$\text{Im}\Sigma^B(\mathbf{k}s, E) = -\frac{K_0}{4} |E| e^{-\frac{\xi^2}{2}\left(k^2 + \frac{E^2}{\hbar^2 v_f^2}\right)} \left[I_0\left(\frac{\xi^2 k E}{\hbar v_f}\right) + s I_1\left(\frac{\xi^2 k E}{\hbar v_f}\right) \right] \tag{S9}$$

For the limit $k, \frac{E}{\hbar v_f} \ll \frac{1}{\xi}$, the above result can be expanded using Eq.(S6) as

$$\begin{aligned}
\text{Im}\Sigma^B(\mathbf{k}s, E) &= -\frac{K_0}{4} |E| \left[1 - \frac{\xi^2}{2} \left(k^2 + \frac{E^2}{\hbar^2 v_f^2} \right) + O(k^4, E^4, k^2 E^2) \right] \left[1 + s \frac{\xi^2 k E}{2\hbar v_f} + O(k^2 E^2) \right] \\
&= -\frac{K_0 |E|}{4} \left[1 - \frac{\xi^2}{2} \left(k^2 + \frac{E^2}{\hbar^2 v_f^2} \right) + \frac{s \xi^2 k E}{2\hbar v_f} \right] + O(k^4, E^4, k^2 E^2) \\
&= -\frac{K_0 |E|}{4} + O(k E^2, k^2 E, E^3)
\end{aligned} \tag{S10}$$

which is the Eq.(17) in the main paper.

For the limit $k, \frac{E}{\hbar v_f} \gg \frac{1}{\xi}$, it has following asymptotic expression by using Eq.(S7)

$$\begin{aligned}
\text{Im}\Sigma^B(\mathbf{k}s, E) &= -\frac{K_0}{4} |E| e^{-\frac{\xi^2}{2}\left(k^2 + \frac{E^2}{\hbar^2 v_f^2}\right)} e^{\frac{\xi^2 k |E|}{\hbar v_f}} \sqrt{\frac{\hbar v_f}{2\pi \xi^2 k |E|}} [1 + s \text{sgn}(E)] \\
&= -\frac{K_0}{4} |E| e^{-\frac{\xi^2}{2}\left(k - \frac{|E|}{\hbar v_f}\right)^2} \sqrt{\frac{\hbar v_f}{2\pi \xi^2 k |E|}} [1 + s \text{sgn}(E)] \\
&\approx -\frac{K_0 (\hbar v_f)^2}{2\xi^2} \delta(E - E_{\mathbf{k}s})
\end{aligned} \tag{S11}$$

where $\text{sgn}(E)$ is signum function of E . The exponential decay term $e^{-\frac{\xi^2}{2}\left(k - \frac{|E|}{\hbar v_f}\right)^2}$ and the term $[1 + s \text{sgn}(E)]$ in the above at the second equation imply that the on-shell approximation ($E = E_{\mathbf{k}s} = s\hbar v_f k$) is valid in this condition. The value of $\text{Im}\Sigma^B$ we obtained under the on-shell approximation is a momentum and energy independent constant.

The corresponding real part of self-energy function can be calculated by the Kramer-Kronig relation,

$$\begin{aligned}
\text{Re}\Sigma^B(\mathbf{k}s, E) &= \frac{1}{\pi} \mathcal{P} \int_{-E_c}^{E_c} dE' \frac{\text{Im}\Sigma^B(\mathbf{k}s, E')}{E' - E} \\
&= \frac{1}{\pi} \mathcal{P} \int_{-E_c}^{E_c} dE' \frac{-\frac{K_0}{4} |E| e^{-\frac{\xi^2}{2}\left(k^2 + \frac{E'^2}{\hbar^2 v_f^2}\right)} \left[I_0\left(\frac{\xi^2 k E}{\hbar v_f}\right) + s I_1\left(\frac{\xi^2 k E}{\hbar v_f}\right) \right]}{E' - E}
\end{aligned} \tag{S12}$$

which is equivalent to the Eq.(16) in the main paper.

For the limit $k, \frac{E}{\hbar v_f} \ll \frac{1}{\xi}$, the corresponding real part of self-energy function is

$$\text{Re}\Sigma^B(\mathbf{k}s, E) = \frac{K_0}{2\pi} E \ln \left| \frac{E}{\hbar v_f k_c} \right| + \alpha E - s \alpha \hbar v_f k + O(k E^2 \ln E, k^2 E \ln E, E^3 \ln E) \tag{S13}$$

which is the Eq.(18) in the main paper. Then combining Eq.(S11) and (S12), we can obtain $\text{Re}\Sigma^B$ at the limit $k, \frac{E}{\hbar v_f} \gg \frac{1}{\xi}$ as

$$\text{Re}\Sigma^B(\mathbf{k}s, E) \approx \frac{K_0 (\hbar v_f)^2}{2\pi} \frac{E - E_{\mathbf{k}s}}{\xi^2 (E - E_{\mathbf{k}s})^2 + (\hbar v_f)^2} \tag{S14}$$

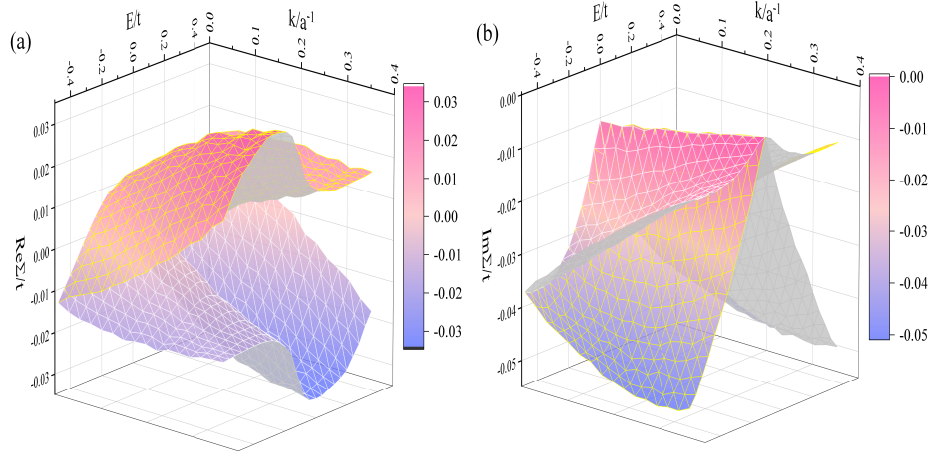


FIG. S1. (Color online). A global dependence of real (a) and imaginary (b) part of self-energy on k and E with same parameters of Fig. 1 in main paper. The surface with yellow grid represents the subband of $s = -1$ and the white grid represents $s = 1$.

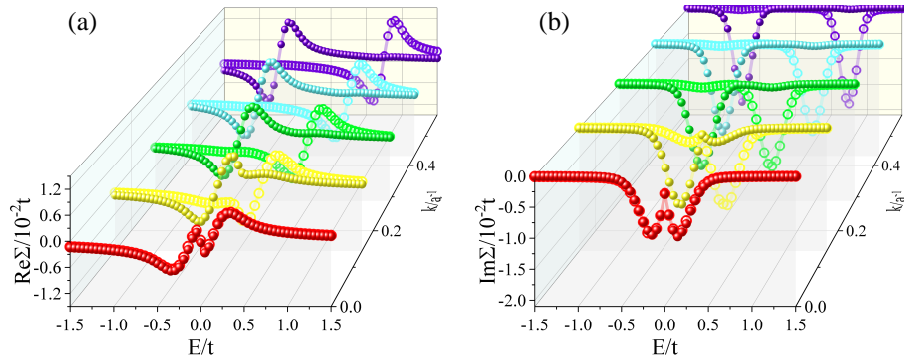


FIG. S2. (Color online). Numerical results of $\text{Re}\Sigma$ (a) and $\text{Im}\Sigma$ (b) vs E with different momentum: $k = 0$ (red), $k = 0.144/a$ (yellow), $k = 0.288/a$ (green), $k = 0.432/a$ (cyan), $k = 0.576/a$ (purple). Lines with solid dots denote subband with $s = -1$ while lines with open dots denote $s = 1$. Other parameters: correlation length $\xi = 10a$, impurity concentration $n_{\text{imp}} = 1\%$, and impurity strength $u_0 = 0.04t$.

NUMERICAL RESULTS OF SELF-ENERGY FUNCTION

In the main paper, we have shown the numerical results of $\text{Re}\Sigma/\text{Im}\Sigma$ vs E with different k and $\text{Re}\Sigma/\text{Im}\Sigma$ vs k with different E . Here, we add the corresponding 3-dimensional global picture shown in Fig. S1.

On the other hand, in order to verify analytical prediction of self-energy at the limit $k, E \gg \frac{1}{\xi}$, i.e. Eq. (S11) and Eq. (S14), we numerically calculate the self-energy function with a large correlation length $\xi = 10a$, as shown in Fig. S2. For the small E and k , where the condition $k, E \ll \frac{1}{\xi}$ still satisfied, the behaviors of the $\text{Re}\Sigma$ and $\text{Im}\Sigma$ are well agree with those exhibited in the main paper. On the contrary, for the large E and k , $\text{Im}\Sigma$ tends to be a delta function which is consistent with the prediction from Born approximation Eq. (S11). Similarly, $\text{Re}\Sigma$ is also consistent with the analytical expression Eq. (S14).

KUBO FORMALISM FOR BUBBLE DIAGRAM AND VERTEX CORRECTION OF CONDUCTIVITY

The self-energy diagram (bubble diagram) of dc conductivity as shown in Fig. S3(a) can be calculated by

$$\sigma_{xx}^0(E) = \sigma_{xx}^{0,RA}(E) - \text{Re}[\sigma_{xx}^{0,RR}(E)] \quad (\text{S15})$$

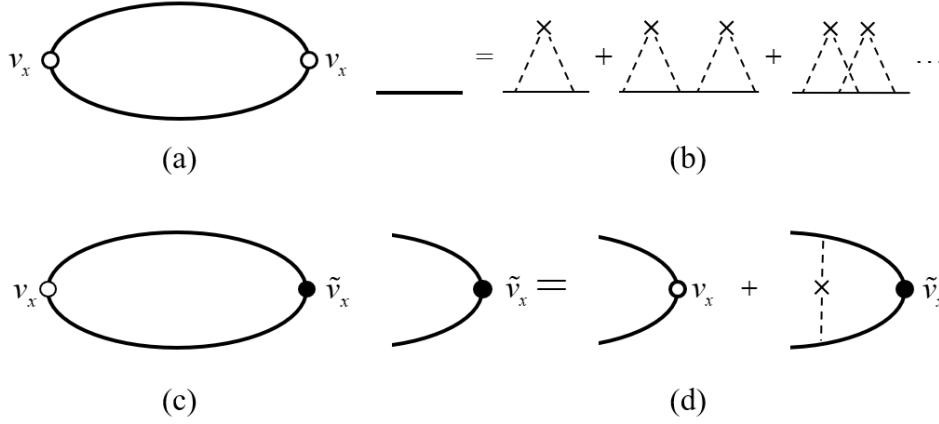


FIG. S3. (a) The self-energy diagram (bubble diagram) of dc conductivity. (b) The self-energy modified Green's function. (c) The vertex corrected diagram of dc conductivity. (d) The “dressed” vertex.

with

$$\sigma_{xx}^{0,RA}(E) = 4 \frac{e^2 \hbar}{2\pi} \int \frac{d^2 \mathbf{k}}{(2\pi)^2} \text{Tr} [G^R(\mathbf{k}, E) v_x(\mathbf{k}) G^A(\mathbf{k}, E) v_x(\mathbf{k})] \quad (\text{S16})$$

$$\sigma_{xx}^{0,RR}(E) = 4 \frac{e^2 \hbar}{2\pi} \int \frac{d^2 \mathbf{k}}{(2\pi)^2} \text{Tr} [G^R(\mathbf{k}, E) v_x(\mathbf{k}) G^R(\mathbf{k}, E) v_x(\mathbf{k})] \quad (\text{S17})$$

Here the factor 4 denotes degeneracy of spin and valley and $\text{Tr}[\dots]$ means the trace in chiral basis. We do the calculation in the eigen basis of pseudospin so that the velocity operator and Green's function are expressed as

$$v_x(\mathbf{k}) = v_f (\cos \theta_{\mathbf{k}} \sigma_z + \sin \theta_{\mathbf{k}} \sigma_y) = v_f \begin{pmatrix} \cos \theta_{\mathbf{k}} & -i \sin \theta_{\mathbf{k}} \\ i \sin \theta_{\mathbf{k}} & -\cos \theta_{\mathbf{k}} \end{pmatrix} \quad (\text{S18})$$

and

$$G^L(\mathbf{k}, E) = \begin{pmatrix} \frac{1}{E - E_{\mathbf{k}+} - \Sigma(\mathbf{k}+, E)} & 0 \\ 0 & \frac{1}{E - E_{\mathbf{k}-} - \Sigma(\mathbf{k}-, E)} \end{pmatrix} = \begin{pmatrix} g_+^L(\mathbf{k}, E) & 0 \\ 0 & g_-^L(\mathbf{k}, E) \end{pmatrix} \quad (\text{S19})$$

where $L = R, A$ denotes the retarded or advanced Green's function and $E_{\mathbf{k}\pm} = \pm \hbar v_f k$ is the eigenvalue. Plugging Eq.(S18) and Eq.(S19) into Eq.(S16) and Eq.(S17), the value of $\sigma_{xx}^{0,RA}$ ($\sigma_{xx}^{0,RR}$) is evaluated

$$\begin{aligned} \sigma_{xx}^{0,LM}(E) &= \frac{2e^2 \hbar v_f^2}{\pi} \int \frac{d^2 \mathbf{k}}{(2\pi)^2} \text{Tr} \left[\begin{pmatrix} g_+^L & 0 \\ 0 & g_-^L \end{pmatrix} \begin{pmatrix} \cos \theta_{\mathbf{k}} & -i \sin \theta_{\mathbf{k}} \\ i \sin \theta_{\mathbf{k}} & -\cos \theta_{\mathbf{k}} \end{pmatrix} \begin{pmatrix} g_+^M & 0 \\ 0 & g_-^M \end{pmatrix} \begin{pmatrix} \cos \theta_{\mathbf{k}} & -i \sin \theta_{\mathbf{k}} \\ i \sin \theta_{\mathbf{k}} & -\cos \theta_{\mathbf{k}} \end{pmatrix} \right] \\ &= \frac{2e^2 \hbar v_f^2}{\pi} \int \frac{d^2 \mathbf{k}}{(2\pi)^2} [\cos^2 \theta_{\mathbf{k}} (g_+^L g_+^M + g_-^L g_-^M) + \sin^2 \theta_{\mathbf{k}} (g_+^L g_-^M + g_-^L g_+^M)] \\ &= \frac{e^2 \hbar v_f^2}{\pi} \int \frac{k dk}{2\pi} [g_+^L g_+^M + g_-^L g_-^M + g_+^L g_-^M + g_-^L g_+^M] \\ &= \frac{e^2 \hbar v_f^2}{\pi} \int \frac{k dk}{2\pi} (g_+^L + g_-^L)(g_+^M + g_-^M) \end{aligned} \quad (\text{S20})$$

where $L, M = R, A$. Since we assume the self-energy function depending on both energy and magnitude of wave vector as

$$\Sigma(\mathbf{k}s, E) = \Sigma_1(E) - s \alpha \hbar v_f k + i \Sigma_2(E), \quad (\text{S21})$$

the full Green's functions can be written as

$$g_+^R(\mathbf{k}, E) = \frac{1}{E - \hbar v_f k - \text{Re}\Sigma(E, k+) - i\text{Im}\Sigma(E, k+)} = \frac{1}{a - (1 - \alpha)v_f \hbar k + i\eta} \quad (\text{S22})$$

$$g_-^R(\mathbf{k}, E) = \frac{1}{E + \hbar v_f k - \text{Re}\Sigma(E, k-) - i\text{Im}\Sigma(E, k-)} = \frac{1}{a + (1 - \alpha)v_f \hbar k + i\eta} \quad (\text{S23})$$

$$g_+^A(\mathbf{k}, E) = \frac{1}{E - \hbar v_f k - \text{Re}\Sigma(E, k+) + i\text{Im}\Sigma(E, k+)} = \frac{1}{a - (1 - \alpha)v_f \hbar k - i\eta} \quad (\text{S24})$$

$$g_-^A(\mathbf{k}, E) = \frac{1}{E + \hbar v_f k - \text{Re}\Sigma(E, k-) + i\text{Im}\Sigma(E, k-)} = \frac{1}{a + (1 - \alpha)v_f \hbar k - i\eta} \quad (\text{S25})$$

$$(\text{S26})$$

with

$$\begin{cases} a = E - \Sigma_1(E) \\ \eta = -\Sigma_2(E) \end{cases} \quad (\text{S27})$$

Therefore we can obtain $\sigma_{xx}^{0,RA}(E)$ and $\text{Re}\sigma_{xx}^{0,RR}(E)$ as

$$\begin{aligned} \sigma_{xx}^{0,RA}(E) &= \frac{e^2 \hbar v_f^2}{\pi} \int \frac{k dk}{2\pi} \left[\frac{1}{a - (1 - \alpha)\hbar v_f k + i\eta} + \frac{1}{a + (1 - \alpha)\hbar v_f k + i\eta} \right] \\ &\quad \left[\frac{1}{a - (1 - \alpha)\hbar v_f k - i\eta} + \frac{1}{a + (1 - \alpha)\hbar v_f k - i\eta} \right] \\ &= \frac{e^2 \hbar v_f^2}{\pi} \int \frac{k dk}{2\pi} \frac{2(a + i\eta)}{(a + i\eta)^2 - (1 - \alpha)^2 (\hbar v_f k)^2} \frac{2(a - i\eta)}{(a - i\eta)^2 - (1 - \alpha)^2 (\hbar v_f k)^2} \\ &= \frac{2e^2}{\pi \hbar} \frac{1}{(1 - \alpha)^2} (a^2 + \eta^2) \int_{\eta^2 - a^2}^{\infty} dx \frac{1}{x^2 + 4a^2 \eta^2} \\ &= \frac{2e^2}{\pi \hbar} \frac{1}{(1 - \alpha)^2} \left(\frac{a}{\eta} + \frac{\eta}{a} \right) \arctan \frac{a}{\eta} \end{aligned} \quad (\text{S28})$$

and

$$\begin{aligned} \text{Re}\sigma_{xx}^{0,RR}(E) &= \text{Re} \frac{e^2 \hbar v_f^2}{\pi} \int \frac{k dk}{2\pi} \left[\frac{1}{a - (1 - \alpha)\hbar v_f k + i\eta} + \frac{1}{a + (1 - \alpha)\hbar v_f k + i\eta} \right]^2 \\ &= \text{Re} \frac{2e^2}{\pi \hbar} \frac{1}{(1 - \alpha)^2} \int dx \frac{(a + i\eta)^2}{[(a + i\eta)^2 - x]^2} \\ &= \frac{2e^2}{\pi \hbar} \frac{1}{(1 - \alpha)^2} \frac{(a + i\eta)^2}{(a + i\eta)^2 - x} \Big|_0^{\infty} \\ &= -\frac{2e^2}{\pi \hbar} \frac{1}{(1 - \alpha)^2} \end{aligned} \quad (\text{S29})$$

Thus the total bubble conductivity is

$$\sigma_{xx}^0(E) = \sigma_{xx}^{0,RA}(E) - \text{Re}[\sigma_{xx}^{0,RR}(E)] = \frac{2e^2}{\pi \hbar} \frac{1}{(1 - \alpha)^2} \left[1 + \left(\frac{a}{\eta} + \frac{\eta}{a} \right) \arctan \frac{a}{\eta} \right] \quad (\text{S30})$$

from which we can obtain minimal conductivity at the limit $E \rightarrow 0$

$$\sigma_{\min}^0 = \frac{2e^2}{\pi \hbar} \frac{1}{(1 - \alpha)^2} \left[1 + \frac{\eta a}{a \eta} \right] = \frac{4}{\pi} \frac{e^2}{\hbar} \frac{1}{(1 - \alpha)^2} \quad (\text{S31})$$

The vertex correction of dc conductivity as shown in Fig. S3(c)(d), can be calculated by

$$\sigma_{xx}^v(E) = \sigma_{xx}^{v,RA}(E) - \text{Re}[\sigma_{xx}^{v,RR}(E)] \quad (\text{S32})$$

with

$$\sigma_{xx}^{v,RA}(E) = 4 \frac{e^2 \hbar}{2\pi} \int \frac{d^2 \mathbf{k}}{(2\pi)^2} \text{Tr} [G^R(\mathbf{k}, E) v_x(\mathbf{k}) G^A(\mathbf{k}, E) \tilde{v}_x^{RA}(\mathbf{k})] \quad (\text{S33})$$

$$\sigma_{xx}^{v,RR}(E) = 4 \frac{e^2 \hbar}{2\pi} \int \frac{d^2 \mathbf{k}}{(2\pi)^2} \text{Tr} [G^R(\mathbf{k}, E) v_x(\mathbf{k}) G^R(\mathbf{k}, E) \tilde{v}_x^{RR}(\mathbf{k})] \quad (\text{S34})$$

Here, the ‘‘dressed’’ vertex function \tilde{v}_x^{LM} is defined by self-consistent Bethe-Salpeter equation

$$\tilde{v}_x^{LM}(\mathbf{k}, E) = v_x(\mathbf{k}) + \int \frac{d^2\mathbf{k}'}{(2\pi)^2} \mathcal{K}(\mathbf{k} - \mathbf{k}') U_{\mathbf{k}}^\dagger U_{\mathbf{k}'} G^L(\mathbf{k}', E) \tilde{v}_x^{LM}(\mathbf{k}, E) G^M(\mathbf{k}', E) U_{\mathbf{k}'}^\dagger U_{\mathbf{k}} \quad (\text{S35})$$

where $U_{\mathbf{k}}^\dagger U_{\mathbf{k}'}$ denotes the spin rotation while momentum changing

$$U_{\mathbf{k}}^\dagger U_{\mathbf{k}'} = \frac{1}{2} \begin{pmatrix} 1 + e^{i\theta} & 1 - e^{i\theta} \\ 1 - e^{i\theta} & 1 + e^{i\theta} \end{pmatrix} \quad (\text{S36})$$

with $\theta = \theta_{\mathbf{k}'} - \theta_{\mathbf{k}}$. In order to solve this self-consistent equation, we at first consider the first order approximation in the following

$$\begin{aligned} \tilde{v}_x^{(1),LM}(\mathbf{k}, E) &= v_x(\mathbf{k}) + \int \frac{d^2\mathbf{k}'}{(2\pi)^2} \mathcal{K}(\mathbf{k} - \mathbf{k}') U_{\mathbf{k}}^\dagger U_{\mathbf{k}'} G^L(\mathbf{k}', E) v_x(\mathbf{k}) G^M(\mathbf{k}', E) U_{\mathbf{k}'}^\dagger U_{\mathbf{k}} \\ &= v_x(\mathbf{k}) + v_f \int \frac{d^2\mathbf{k}'}{(2\pi)^2} \frac{\mathcal{K}(\mathbf{k} - \mathbf{k}')}{4} \begin{pmatrix} 1 + e^{i\theta} & 1 - e^{i\theta} \\ 1 - e^{i\theta} & 1 + e^{i\theta} \end{pmatrix} \begin{pmatrix} g_+^L & \\ & g_-^L \end{pmatrix} \begin{pmatrix} \cos \theta_{\mathbf{k}'} & -i \sin \theta_{\mathbf{k}'} \\ i \sin \theta_{\mathbf{k}'} & -\cos \theta_{\mathbf{k}'} \end{pmatrix} \\ &\quad \begin{pmatrix} g_+^M & \\ & g_-^M \end{pmatrix} \begin{pmatrix} 1 + e^{-i\theta} & 1 - e^{-i\theta} \\ 1 - e^{-i\theta} & 1 + e^{-i\theta} \end{pmatrix} \\ &= v_x(\mathbf{k}) + v_f \int \frac{d^2\mathbf{k}'}{(2\pi)^2} \frac{\mathcal{K}(\mathbf{k} - \mathbf{k}')}{4} \begin{pmatrix} M_{11} & M_{12} \\ M_{21} & M_{22} \end{pmatrix} \end{aligned} \quad (\text{S37})$$

where the expressions of $M_{ss'}$ are in the following

$$\begin{aligned} M_{11} &= 2 \cos \theta (g_+^L g_+^M - g_-^L g_-^M) \cos \theta_{\mathbf{k}} + [2 \cos^2 \theta (g_+^L g_+^M + g_-^L g_-^M) + 2 \sin^2 \theta (g_+^L g_-^M + g_-^L g_+^M)] \cos \theta_{\mathbf{k}} \\ M_{22} &= 2 \cos \theta (g_+^L g_+^M - g_-^L g_-^M) \cos \theta_{\mathbf{k}} + [2 \cos^2 \theta (g_+^L g_+^M + g_-^L g_-^M) + 2 \sin^2 \theta (g_+^L g_-^M + g_-^L g_+^M)] (-\cos \theta_{\mathbf{k}}) \\ M_{12} &= 2i \cos \theta (g_+^L g_-^M - g_-^L g_+^M) \sin \theta_{\mathbf{k}} + [2 \cos^2 \theta (g_+^L g_+^M + g_-^L g_-^M) + 2 \sin^2 \theta (g_+^L g_-^M + g_-^L g_+^M)] (-i \sin \theta_{\mathbf{k}}) \\ M_{21} &= 2i \cos \theta (g_+^L g_-^M - g_-^L g_+^M) \sin \theta_{\mathbf{k}} + [2 \cos^2 \theta (g_+^L g_+^M + g_-^L g_-^M) + 2 \sin^2 \theta (g_+^L g_-^M + g_-^L g_+^M)] (i \sin \theta_{\mathbf{k}}) \end{aligned} \quad (\text{S38})$$

Based on the expressions of $M_{ss'}$, we can rewrite $\tilde{v}_x^{(1),LM}(\mathbf{k}, E)$ as

$$\frac{\tilde{v}_x^{(1),LM}(\mathbf{k}, E)}{v_f} = f_0^{LM}(\mathbf{k}, E) \cos \theta_{\mathbf{k}} \sigma_0 + f_x^{LM}(\mathbf{k}, E) \sin \theta_{\mathbf{k}} \sigma_x + f_y^{LM}(\mathbf{k}, E) \sin \theta_{\mathbf{k}} \sigma_y + f_z^{LM}(\mathbf{k}, E) \cos \theta_{\mathbf{k}} \sigma_z \quad (\text{S39})$$

For $\tilde{v}_x^{(1),RA}(\mathbf{k}, E)$, the functions $f_i^{RA}(\mathbf{k}, E)$ with $(i = 0, x, y, z)$ are

$$\begin{aligned} f_0^{RA}(\mathbf{k}, E) &= \int \frac{d^2\mathbf{k}'}{(2\pi)^2} \frac{\mathcal{K}(\mathbf{k} - \mathbf{k}')}{2} \cos \theta (g_+^R g_+^A - g_-^R g_-^A) \\ &\approx \frac{K_0 (\hbar v_f)^2}{8\pi^2} \int k' dk' d\theta \left[1 - \frac{\xi^2}{2} (k^2 + k'^2) + \xi^2 k k' \cos \theta \right] \cos \theta (g_+^R g_+^A - g_-^R g_-^A) \\ &\approx \frac{K_0 \xi^2 a}{4\pi (1 - \alpha)^3 \hbar v_f} \ln \left(\frac{E_c^2}{a^2 + \eta^2} \right) k \end{aligned} \quad (\text{S40})$$

$$\begin{aligned} f_x^{RA}(\mathbf{k}, E) &= \int \frac{d^2\mathbf{k}'}{(2\pi)^2} \frac{\mathcal{K}(\mathbf{k} - \mathbf{k}')}{2} i \cos \theta (g_{0,+}^R g_{0,-}^A - g_{0,-}^R g_{0,+}^A) \\ &\approx \frac{K_0 (\hbar v_f)^2}{8\pi^2} \int k' dk' d\theta \left[1 - \frac{\xi^2}{2} (k^2 + k'^2) + \xi^2 k k' \cos \theta \right] i \cos \theta (g_+^R g_-^A - g_-^R g_+^A) \\ &\approx \frac{K_0 \xi^2 \eta}{4\pi (1 - \alpha)^3 \hbar v_f} \ln \left(\frac{E_c^2}{a^2 + \eta^2} \right) k \end{aligned} \quad (\text{S41})$$

$$\begin{aligned} f_y^{RA}(\mathbf{k}, E) = f_z^{RA}(\mathbf{k}, E) &= 1 + \int \frac{d^2\mathbf{k}'}{(2\pi)^2} \frac{\mathcal{K}(\mathbf{k} - \mathbf{k}')}{2} [\cos^2 \Delta \theta (g_+^L g_+^M + g_-^L g_-^M) + \sin^2 \Delta \theta (g_+^L g_-^M + g_-^L g_+^M)] \\ &\approx 1 + \frac{K_0 (\hbar v_f)^2}{8\pi} \int k' dk' (g_+^L g_+^M + g_-^L g_-^M + g_+^L g_-^M + g_-^L g_+^M) \\ &\approx 1 + \frac{K_0}{4\pi (1 - \alpha)^2} \left(\frac{a}{\eta} + \frac{\eta}{a} \right) \arctan \frac{a}{\eta} \end{aligned} \quad (\text{S42})$$

For $\tilde{v}_x^{RR}(\mathbf{k}, E)$, the functions $f_i^{RR}(\mathbf{k}, E)$ with $(i = 0, x, y, z)$ are

$$\begin{aligned} f_0^{RR}(\mathbf{k}, E) &= \int \frac{d^2\mathbf{k}'}{(2\pi)^2} \frac{\mathcal{K}(\mathbf{k} - \mathbf{k}')}{2} \cos\theta(g_+^R g_+^R - g_-^R g_-^R) \\ &\approx \frac{K_0(\hbar v_f)^2}{8\pi^2} \int k' dk' d\theta \left[1 - \frac{\xi^2}{2}(k^2 + k'^2) + \xi^2 k k' \cos\theta \right] \cos\theta(g_+^R g_+^R - g_-^R g_-^R) \\ &\approx \frac{K_0 \xi^2 (a + i\eta)}{4\pi(1 - \alpha)^3 \hbar v_f} \ln\left(\frac{E_c^2}{a^2 + \eta^2}\right) k \end{aligned} \quad (\text{S43})$$

$$f_x^{RR}(\mathbf{k}, E) = \int \frac{d^2\mathbf{k}'}{(2\pi)^2} \frac{\mathcal{K}(\mathbf{k} - \mathbf{k}')}{2} i \cos\theta(g_+^R g_-^R - g_-^R g_+^R) = 0 \quad (\text{S44})$$

$$\begin{aligned} f_y^{RR}(\mathbf{k}, E) = f_z^{RR}(\mathbf{k}, E) &= 1 + \int \frac{d^2\mathbf{k}'}{(2\pi)^2} \frac{\mathcal{K}(\mathbf{k} - \mathbf{k}')}{2} [\cos^2\theta(g_+^R g_+^R + g_-^R g_-^R) + \sin^2\theta(g_+^R g_-^R + g_-^R g_+^R)] \\ &\approx 1 + \frac{K_0(\hbar v_f)^2}{8\pi} \int k' dk' (g_+^R g_+^R + g_-^R g_-^R + g_+^R g_-^R + g_-^R g_+^R) \\ &\approx 1 - \frac{K_0}{4\pi(1 - \alpha)^2} \end{aligned} \quad (\text{S45})$$

Plugging Eqs.(S40)-(S45) into Eqs.(S39), (S33), and (S34), we can get the first-order $\sigma_{xx}^{v,RA}$ and $\text{Re}(\sigma_{xx}^{v,RR})$ as

$$\begin{aligned} \sigma_{xx}^{(1),RA}(E) &= \frac{e^2 \hbar v_f^2}{2\pi^2} \int k dk \left[1 + \frac{K_0}{4\pi(1 - \alpha)^2} \left(\frac{a}{\eta} + \frac{\eta}{a}\right) \arctan \frac{a}{\eta} \right] (g_+^R g_+^A + g_-^R g_-^A + g_+^R g_-^A + g_-^R g_+^A) \\ &\quad + \frac{K_0 \xi^2 a}{4\pi(1 - \alpha)^3 \hbar v_f} \ln\left(\frac{E_c^2}{a^2 + \eta^2}\right) k (g_+^R g_+^A - g_-^R g_-^A) - i \frac{K_0 \xi^2 \eta}{4\pi(1 - \alpha)^3 \hbar v_f} \ln\left(\frac{E_c^2}{a^2 + \eta^2}\right) k (g_+^R g_-^A - g_-^R g_+^A) \\ &= \frac{2e^2}{\pi h} \left\{ \left(\frac{a}{\eta} + \frac{\eta}{a}\right) \arctan \frac{a}{\eta} \left[1 + \frac{K_0}{4\pi(1 - \alpha)^4} \left(\frac{a}{\eta} + \frac{\eta}{a}\right) \arctan \frac{a}{\eta} \right] + \frac{K_0 \xi^2 (a^2 - \eta^2)}{4\pi(\hbar v_f)^2} \left[\frac{1}{(1 - \alpha)^3} \ln\left(\frac{E_c^2}{a^2 + \eta^2}\right) \right]^2 \right\} \end{aligned} \quad (\text{S46})$$

and

$$\begin{aligned} \text{Re}[\sigma_{xx}^{(1),RR}(E)] &= \frac{e^2 \hbar v_f^2}{2\pi^2} \text{Re} \int k dk \left[1 - \frac{K_0}{4\pi(1 - \alpha)^2} \right] (g_+^R g_+^R + g_-^R g_-^R + g_+^R g_-^R + g_-^R g_+^R) \\ &\quad + \frac{K_0 \xi^2 (a + i\eta)}{4\pi(1 - \alpha)^3 \hbar v_f} \ln\left(\frac{E_c^2}{a^2 + \eta^2}\right) k (g_+^R g_+^R - g_-^R g_-^R) \\ &= \frac{2e^2}{\pi h} \left\{ -1 + \frac{K_0}{4\pi(1 - \alpha)^4} + \frac{K_0 \xi^2 (a^2 - \eta^2)}{4\pi(\hbar v_f)^2} \left[\frac{1}{(1 - \alpha)^3} \ln\left(\frac{E_c^2}{a^2 + \eta^2}\right) \right]^2 \right\} \end{aligned} \quad (\text{S47})$$

where $E_c = \hbar v_f k_c$. Thus the first-order vertex correction of dc conductivity is obtained as

$$\begin{aligned} \sigma_{xx}^{(1)}(E) &= \sigma_{xx}^{(1),RA}(E) - \text{Re}[\sigma_{xx}^{(1),RR}(E)] \\ &= \frac{2e^2}{\pi h} \left[1 + \left(\frac{a}{\eta} + \frac{\eta}{a}\right) \arctan \frac{a}{\eta} \right] + \frac{K_0}{4\pi(1 - \alpha)^4} \left[\left(\frac{a}{\eta} + \frac{\eta}{a}\right) \arctan \frac{a}{\eta} - 1 \right] \end{aligned} \quad (\text{S48})$$

from which we can see that coefficients f_0^{LM} and f_x^{LM} can be ignored in the ‘‘dressed’’ vertex. Thus, we can find that ‘‘dressed’’ vertex has same matrix structure with the bare velocity and can be solved as

$$\begin{aligned} \tilde{v}_x^{RA}(\mathbf{k}, E) &= \frac{1}{1 + \frac{K_0}{4\pi(1 - \alpha)^2} \left(\frac{a}{\eta} + \frac{\eta}{a}\right) \arctan \frac{a}{\eta}} v_f (\cos\theta_{\mathbf{k}} \sigma_z + \sin\theta_{\mathbf{k}} \sigma_y) \\ \tilde{v}_x^{RR}(\mathbf{k}, E) &= \frac{1}{1 - \frac{K_0}{4\pi(1 - \alpha)^2}} v_f (\cos\theta_{\mathbf{k}} \sigma_z + \sin\theta_{\mathbf{k}} \sigma_y) \end{aligned} \quad (\text{S49})$$

Based on this corrected vertex, the total dc conductivity will arrive at

$$\sigma_{xx}^v(E) = \frac{2e^2}{\pi h} \frac{1}{(1 - \alpha)^2} \left[\frac{1}{1 - \frac{K_0}{4\pi(1 - \alpha)^2}} + \frac{\left(\frac{a}{\eta} + \frac{\eta}{a}\right) \arctan \frac{a}{\eta}}{1 + \frac{K_0}{4\pi(1 - \alpha)^2} \left(\frac{a}{\eta} + \frac{\eta}{a}\right) \arctan \frac{a}{\eta}} \right] \quad (\text{S50})$$

and the corresponding vertex corrected minimal conductivity is

$$\sigma_{\min}^v = \frac{4e^2}{\pi h} \frac{1}{(1-\alpha)^2} \frac{1}{1 - \left[\frac{K_0}{4\pi(1-\alpha)^2} \right]^2} \xrightarrow{K_0 \lesssim 1} \frac{4e^2}{\pi h} \frac{1}{(1-\alpha)^2} \quad (\text{S51})$$

Since typical experiment conditions of weak disordered and high mobility graphene correspond to $K_0 \lesssim 1$, the influence of vertex correction to the minimal conductivity is much smaller than those induced by the linear momentum dependent self-energy in the bubble diagram.

* Corresponding author. E-mail: phsqw@ustc.edu.cn

† Corresponding author. E-mail: zhuwei@westlake.edu.cn